

Spontaneous formation of magnetic dipoles by interaction of intense laser with overdense plasma

Devshree Mandal^{1,2,*}, AyushiVashistha^{1,2}, and Amita Das³

¹ *Institute for Plasma Research, HBNI, Bhat, Gandhinagar - 382428, India*

² *Homi Bhabha National Institute, Mumbai, 400094 and*

³ *Physics Department, Indian Institute of Technology Delhi, Hauz Khas, New Delhi - 110016, India*

When a laser radiation is incident on an overdense plasma it is unable to penetrate inside it. Nevertheless, a part of its energy gets transferred to the electrons. The dynamics of these energetic electrons inside the plasma is often a field of great interest. It has often been conjectured that the dynamics of the electrons in the plasma can be suitably described by the Electron Magnetohydrodynamic (EMHD) prescription. It is demonstrated here using PIC (Particle - In - Cell) simulation studies with the help of Osiris4.0 framework that this is indeed true. In 2-D simulations we observe a spontaneous formation of a variety of coherent solutions which essentially follow the dynamics of EMHD and its generalized fluid descriptions. We discuss the conditions for the formation of such structures and also identify their particulate kinetic behaviour in this study.

I. INTRODUCTION

Interaction of laser with plasma has always been an alluring topic with rich physical aspects. Depending on laser parameters, various aspects of laser plasma interaction has been successfully implied in numerous applications ranging from medical therapy[1–5], nonlinear optics[5–8] to inertial confinement fusion[9–11]. The immense potential associated with this generates considerable interest in its study and research. Such wide variety of applications have come up because the laser radiation can easily get the plasma response to be nonlinear. There are several interesting non-linear phenomena which bear testimony to this. The excitation of nonlinear wakefield structures, soliton formation, stimulated Raman scattering, laser focusing etc, are some which have been observed and widely studied. While most of these listed are for a plasma which is underdense with respect to the laser radiation. The laser radiation continues to propagate in an underdense plasma medium and interacts with the bulk of the plasma medium in these cases. In the context of overdense plasma, the laser energy gets dumped around the critical density layer. The laser energy gets partly absorbed by the plasma electrons. These energetic electrons then interact with the rest of the plasma and elicit its response in various forms.

We demonstrate here, with the help of 2-D Particle - In - Cell (PIC) simulations that the energetic electrons created by the laser organize with the plasma electrons to spontaneously form 2-D coherent structures. These coherent structures are shown to exhibit characteristics features of nonlinear coherent solutions permitted by the Electron Magnetohydrodynamics (EMHD) model.

The Electron Magnetohydrodynamic (EMHD) model essentially describes the dynamics of magnetized electron

fluid for which the time scales of interest are fast enough to ignore ion motion [12, 13] and considerably slower to ignore the displacement current contribution. The EMHD model permits certain coherent nonlinear exact solutions of monopolar and dipole vortex forms which are quite robust and stable. While the monopole vortices are stationary, the dipoles propagate along their axis in a plasma with homogeneous density. When the plasma density is varying both monopoles and dipoles acquire an additional drift velocity and display interesting dynamical traits. The dynamics of these structures have been studied in detail with the help of fluid simulations by Das et al.[14] in the context of homogenous plasma and by Sharad et al.[15] for inhomogeneous plasma. These coherent structures have been perceived to have important implications as they can possibly be utilized for the purpose of transporting energy from laser to overdense regions of plasma. For instance, this could be useful for igniting the compressed fuel in the fast ignition scenario. In fact, it has been shown earlier in the work by Sharad et al.[16] that by appropriately tailoring plasma density inhomogeneity, the path of these structures can be guided and its energy can also be anomalously dissipated at a rate much higher than the permissible limit of classical collisional values[17].

The pertinent question that remains to be answered in this regard is whether such coherent structures can be generated by a laser interaction with an overdense plasma medium and the conditions under which it possibly can be formed. We demonstrate such a possibility by carrying out PIC simulations in the framework of OSIRIS4.0[18–20]. In this context we will like to mention that some earlier studies have also observed the formation of coherent 2-D structures in simulations. Bulanov et al.[21] were the first to show the generation of dipolar structures in the wake of a laser field in an underdense plasma medium. Several attempts have been made to study the formation and propagation of self-excited EMHD dipoles in plasmas. In a recent study[22], external magnetic fields have

*devshreemandal@gmail.com

been employed to guide the magnetic field fluctuations that get generated in the counterstreaming beam plasma systems via Weibel and oblique filamentation instability. The formation of magnetic dipoles have also been observed in wake of near critical density plasmas to equilibrate the huge electric field due to evacuating electrons and the resultant magnetic pressure around the depletion region[23].

In this work, we present a comprehensive study of spontaneous formation and propagation of magnetic dipole vortices in case of intense laser interaction with overdense plasma. It has been shown that dipoles are robust in shallower density profiles of plasma and they propagate faster in the sharper density gradients. Particle trajectories reveal the interesting kinetic behaviour of electrons in dipole vortices which also has been presented here.

Section II discusses simulation details which has been used in this paper. Section III describe results in details and in various subsections we show various aspects of the magnetic dipole vortices and concluding remarks are shown in section IV.

II. SIMULATION DETAILS

We have employed OSIRIS 4.0 framework to carry out Particle - In - Cell (PIC) simulation [18–20] for our study. We chose a 2-D slab geometry with XY plane as our simulation domain. A square box of side $L = 500d_e$ with 25000×25000 cells is considered ($d_e = c/\omega_{pe}$ is skin depth of the plasma). Fig.1 shows the schematic of simulation geometry. Region I and IV indicates vacuum whereas region II and III contain a plasma slab. Region II has a linearly increasing plasma density profile in \hat{x} which saturates and gives a uniform plasma density in region III. Ions are kept stationary and provide a neutralising background. A p -polarized laser pulse (with electric field lying in the 2-D plane of simulation) is incident normally from left side of the target. The longitudinal profile of

pulse is a polynomial function with rise and fall time of $35 \omega_{pe}^{-1}$ and flat top for $10 \omega_{pe}^{-1}$ while perpendicular profile is Gaussian with $fwhm = 30d_e$. The boundary for particles and electromagnetic fields are absorbing along both directions. Table I presents laser and plasma parameters in normalized units and their corresponding experimental values.

III. RESULTS AND DISCUSSIONS

A. Formation of Dipole vortices

It is well known that a non-relativistic laser incident normally can only penetrate upto a few skin depths of an overdense plasma (*i.e.* $\omega_L < \omega_{pe}$). However, in case of intense pulse (*i.e.* $a_0 > 1$), under the influence of strong electric field of laser pulse electrons gains a directed velocity ($\sim c$) in the system. Thus, pulse is able to propagate deeper than skin depths as effective plasma frequency gets modified due to relativistic effects[24–26]. These energetic electrons accelerating into plasma acts as forward current and background plasma inhibits this strong incoming current by generating a return current in response to it. The interaction of these accelerating electrons with background plasma is highly non-linear. With time, this non-linearity will make its presence known in the form of coherent structures or growth of instabilities in the medium leading to a turbulent state.

We focus our study on formation of one such coherent structure. We observe formation of magnetic field dipoles in plasma upon interaction with an intense laser. The formation of these structures can be attributed to local uncomponation of total current in the bulk plasma which leads to spontaneous generation of high magnetic field structures. It has been observed that the forward current (due to energetic electrons) and return current (plasma response to energetic electrons) broadly compensate each other [27]. However, there always remains some uncomponation of total current in the plasma which sustains itself for a very long time. We plot forward, return and total longitudinal current density of the system (integrated over space) as function of time (fig.2) and observe that although forward and return currents match their orders of magnitude, but there is always a finite total current in the system (inset of fig.2). The reason for this uncomponation can be understood from fig. 3, where we show temporal variation of $\vec{J} \cdot \vec{E}$ of the system. Positive amplitude of $\vec{J} \cdot \vec{E}$ indicates that \vec{J} and \vec{E} are in resistive phase to each other *i.e.* electric power is dissipated by electrons. In other words, Lorentz force acts on electron resulting in heat dissipation which is an irreversible process and this loss of energy can be attributed to the mismatch in forward and return currents. This remanant current in the system then generates magnetic field structures which plays an important role in the spontaneous

TABLE I: A comparison of normalised and experimental values of simulation parameters

Parameters	Normalised Value	values in standard units
Laser Parameters		
Frequency	1	3.2×10^{14} Hz
Wavelength	2.17	$1 \mu\text{m}$
Intensity	$a_0 = 25$	$8 \times 10^{20} \text{ W/cm}^2$
Plasma Parameters		
Number density (n_0)	1	$3.4 \times 10^{20} \text{ cm}^{-3}$
Electron Plasma frequency (ω_{pe})	1	1×10^{15} Hz
Electron skin depth (c/ω_{pe})	1	$0.46 \mu\text{m}$

formation of dipole vortices.

Interaction of an intense laser pulse with overdense plasma leads to generation of high amplitude magnetic field at vacuum-plasma interface extending upto tens of skin depths into bulk plasma. This self-generated magnetic field is susceptible to various instabilities like Weibel, filamentation which separate magnetic field profile into random structures. We observe the same phenomenon in our simulation where a high magnetic field gets generated at vacuum-plasma interface (fig. 4, $t=50$) and further filaments giving rise to smaller magnetic field structures ($t \approx 100$). We observe two opposite polarity field being generated. To achieve electromagnetic equilibrium, same polarity structures combine themselves to form a bigger lobe of magnetic field giving rise to two vortices of opposite polarity. We call one such set of vortices a dipole for their dynamics being coupled to each other. One should note that the laser pulse has to be highly intense to generate such magnetic field structures. For low intensity case, laser will not be able to penetrate inside overdense plasma and will be reflected back from the plasma boundary. We verified this by taking $a_0 = 0.25$ in our simulation and did not observe formation of any such structures in plasma.

B. Role of inhomogeneity on the dynamics of dipole

In the previous section, we explained the formation of magnetic dipoles in plasma. In this section, we demonstrate the effect of plasma density gradient on the dynamics of these structures. Prior to investigating the role of density gradient on dipole dynamics, we studied the dynamics of dipole in uniform density plasma ($\delta n/\delta x = 0.0$) and then compared the results with two varying density gradients ($\delta n/\delta x = 0.05, 0.005$). Fig.4,5,6 show a comparison of the dynamics of dipole for the above mentioned three cases. For a uniform density plasma (fig. 4), these structures are found to be stationary, only rotating about their axis. Their rotatory motion can be attributed to $\vec{E} \times \vec{B}$ force acting on them (details will be discussed in the next section). However, for non-uniform density plasma, $\delta n/\delta x = 0.05$ (referred to as case(A)) and $\delta n/\delta x = 0.005$ (referred to as case(B)), these magnetic dipole structures are found to be propagating along \hat{x} . This suggests that gradient in plasma density helps dipole propagate inside. Further, we examine the effect of varying density gradient on the dynamics of the dipole and found that dipoles formed in case(B) are wider and travel longer distance along \hat{x} than those in case(A) [fig. 6]. This indicates that shallower the gradient, faster the propagation of dipole inside plasma. Therefore, by tuning density gradient one can provide a control over the dynamics of dipole structures.

Our next key observation is the effect of density gradient over the robustness of the dipole structure.

Comparison of case(A) and (B) has been shown in fig. 7 where we show spatial variation of B_z and J_x . The time has been chosen such that dipoles are robust and have not turned their trajectory in both cases [ref fig. 7]. In fig.7, left subplot shows the unbalanced nature of dipole vortices where positive and negative amplitude of B_z do not exactly match. On the other hand, right subplot fig. 7 shows spatial variation of longitudinal current density J_x which is responsible for the formation of dipole structures. Dipole structure has spatially separated forward and reverse shielding current. The central region between positive and negative peak of magnetic field (at $y \approx 248$ for case(A) and $y \approx 253$ in left subplot fig. 7) corresponds to peak value of J_x in right subplot fig. 7.

To establish the robustness of dipole in case(B) and higher translational velocity in case(A), we plot $\langle |B_z| \rangle$ as function of x at different times (ref. fig.8). In case(A), (left subplot of fig.8), amplitude of $\langle |B_z| \rangle$ decreases with time and dipole reaches $x = 155$ in 400 plasma periods. While in case(B), the amplitude of $\langle |B_z| \rangle$ does not change and dipole travels same distance in 1000 plasma periods approximately. Thus dipole structure is found to be more robust and propagate faster in shallower density gradient.

We looked into energy evolution to analyse the exchange of energy. Fig. 9 shows that as laser pulse starts interacting with plasma, kinetic energy of system starts increasing and at around $t \approx 150$ laser has totally reflected back to the left wall of simulation box and hence gets absorbed at wall which explains the abrupt fall of total energy of the system. Also, we observe that after 500 plasma periods, EMF and kinetic energy of electrons saturate, which establishes that the system has reached Electromagnetic equilibrium. The little dip in energies at later time periods is due to absorbing boundary conditions in transverse directions.

C. $\vec{E} \times \vec{B}$ picture of dipole vortex

It has been discussed in the previous section how shallower density gradients help in propagation of dipole in plasma. In this section we address the rotatory motion of dipole structure. These dipole structures are formed by high amplitude magnetic fields of opposite polarity, corresponding to which, there will always be an electric field of the same order. Therefore, their rotatory motion can be explained by the cross product of these two fields. To identify the direction of $\vec{E} \times \vec{B}$, we superpose quiver plot of electric field vector over colorplots of B_z (fig.10). It can be seen that electric field is pointing radially outward (along \hat{r}) and magnetic field being along \hat{z} gives a rotatory motion to dipole along $\hat{\theta}$. The net magnetic field of the dipole structure decides whether the dipole will have a clockwise or an anti-clockwise rotation. Therefore, the larger lobe gets to decide the

direction of rotation of the dipole.

In an inhomogenous plasma, dipole shows both translation as well as rotational motion (fig. 11). After being formed near vacuum-plasma interface, dipole translates for a while and then in an effort to balance the fields in the lobes, it turns around its axis (at $t = 900$) and starts moving along y-axis. After a certain point of time ($t = 2150$), due to rotatory motion dipole experiences a force along $-\hat{x}$, henceforth experiencing a negative density gradient. As there is an additional drift of dipole due to inhomogeneity along $\frac{B\hat{z}\times\hat{\nabla}n}{n^2}$ [16] leading to separation of dipole structure into two monopoles ($t = 2400$).

D. Tracking trajectories of particles in dipole vortex

In this section, an effort to draw kinetic picture of these magnetic field structures has been presented. We choose some particles from the space around dipole structure and track their motion. Temporal evolution of particle kinetic energy has been plotted in fig. 12 and their space evolution has been shown in inset of the same. As can be seen in fig.12(A), particle 1,2,3 remain trapped inside dipole upto $t = 1000$ and their kinetic energy fluctuations also being approximately equal to each other. The motion of these electrons can be seen as a combination of local gyration under the effect of magnetic field and motion around the lobe of dipole itself.

In fig.12(B), we show another interesting category of particles which get trapped inside dipole for a while but get untrapped as soon as they reach the periphery of the dipole. The reason for untrapping being the kinetic energy of these particles exceeds the magnetic field energy at that point. From fig.12(B), we observe that particle 5 and 6 spend about $620(\omega_{pe}^{-1})$ ($t \approx 100$ to $t \approx 720$) and $270(\omega_{pe}^{-1})$ ($t \approx 450$ to $t \approx 720$) time inside dipole respectively. After leaving the vortex both particles move inside plasma without any interruptions. The reason for their motion being unhindered by the background plasma is that they have much higher kinetic energy as compared to the background plasma electrons. Being so highly en-

ergetic, their collision cross-section decreases and they move uninhibitedly inside plasma. This can be a very interesting way to inject highly energetic electrons inside plasma. A detailed study of this striking effect can be done and signatures of this can also be checked in the laboratory experiments.

IV. CONCLUSIONS

We simulated interaction of an intense laser pulse with overdense plasma and observed spontaneous formation of magnetic dipole structures in the system. Uncompensation of forward current (due to energetic electrons) and return current (plasma response to energetic electrons) leads to generation of magnetic field which being susceptible to filamentation breaks into smaller chunks of magnetic field. These small chunks of magnetic field coalesce to form a magnetic dipole structure. The dipole structure so formed is found to be more robust and propagating slower in plasma with shallower density gradients. The rotary motion of dipole is mainly governed by the direction of $\vec{E} \times \vec{B}$. Particle tracking around these structures gave an insight into a very interesting phenomenon where some particles were found to be trapped inside the dipole whereas some get untrapped after sometime. The reason for their untrapping being their high kinetic energy as compared to the magnetic field energy of the structure at that point. The untrapped particles being highly energetic moves unhindered in plasma.

Acknowledgements

The authors would like to acknowledge the OSIRIS Consortium, consisting of UCLA and IST (Lisbon, Portugal) for providing access to the OSIRIS4.0 framework which is the work supported by NSF ACI-1339893. AD would like to acknowledge her J. C. Bose fellowship grant JCB/2017/000055 and the CRG/2018/000624 grant of DST for the work. The simulations for the work described in this paper were performed on Uday, an IPR Linux cluster. DM and AV would like to thank Mr. Omstavan Samant for fruitful discussions at IPR.

References:

-
- [1] KWD Ledingham, P McKenna, T McCanny, S Shimizu, JM Yang, L Robson, Jamal Zweit, James M Gillies, J Bailey, GN Chimon, et al. High power laser production of short-lived isotopes for positron emission tomography. *Journal of Physics D: Applied Physics*, 37(16):2341, 2004.
 - [2] JM Dawson, HC Kim, D Arnush, BD Fried, RW Gould, LO Heflinger, CF Kennel, TE Romesser, RL Stenzel, AY Wong, et al. Isotope separation in plasmas by use of ion cyclotron resonance. *Physical Review Letters*, 37(23):1547, 1976.
 - [3] SD Kraft, C Richter, K Zeil, M Baumann, E Beyreuther, S Bock, M Bussmann, TE Cowan, Y Dammene, W Enghardt, et al. Dose-dependent biological damage of tumour cells by laser-accelerated proton beams. *New Journal of Physics*, 12(8):085003, 2010.
 - [4] SV Bulanov, T Zh Esirkepov, VS Khoroshkov, AV Kuznetsov, and Francesco Pegoraro. Oncological hadrontherapy with laser ion accelerators. *Physics Letters A*, 299(2-3):240–247, 2002.
 - [5] Andrea Macchi, Marco Borghesi, and Matteo Passoni. Ion acceleration by superintense laser-plasma interaction.

- Rev. Mod. Phys.*, 85:751–793, May 2013.
- [6] JJ Su, T Katsouleas, JM Dawson, and R Fedele. Plasma lenses for focusing particle beams. *Physical Review A*, 41(6):3321, 1990.
- [7] S. Weber, C. Riconda, L. Lancia, J.-R. Marquès, G. A. Mourou, and J. Fuchs. Amplification of ultrashort laser pulses by brillouin backscattering in plasmas. *Phys. Rev. Lett.*, 111:055004, Jul 2013.
- [8] L. Lancia, J.-R. Marquès, M. Nakatsutsumi, C. Riconda, S. Weber, S. Hüller, A. Mančić, P. Antici, V. T. Tikhonchuk, A. Héron, P. Audebert, and J. Fuchs. Experimental evidence of short light pulse amplification using strong-coupling stimulated brillouin scattering in the pump depletion regime. *Phys. Rev. Lett.*, 104:025001, Jan 2010.
- [9] M Temporal, JJ Honrubia, and S Atzeni. Numerical study of fast ignition of ablatively imploded deuterium-tritium fusion capsules by ultra-intense proton beams. *Physics of Plasmas*, 9(7):3098–3107, 2002.
- [10] M Roth, TE Cowan, MH Key, SP Hatchett, C Brown, W Fountain, J Johnson, DM Pennington, RA Snavely, SC Wilks, et al. Fast ignition by intense laser-accelerated proton beams. *Physical Review Letters*, 86(3):436, 2001.
- [11] R Kodama, PA Norreys, K Mima, AE Dangor, RG Evans, H Fujita, Y Kitagawa, K Krushelnick, T Miyakoshi, N Miyanaga, et al. Fast heating of ultrahigh-density plasma as a step towards laser fusion ignition. *Nature*, 412(6849):798, 2001.
- [12] Marnachev A. M. Isichenko M. B. *Sov. Phys. JETP*, 66:702, 1987.
- [13] Biskamp D. *Phys. Rev. Lett.*, 76:1264, 1996.
- [14] Das A. *Plasma Phys. Controlled Fusion*, 41:A531, 1999.
- [15] Sharad Kumar Yadav, Amita Das, and Predhiman Kaw. Propagation of electron magnetohydrodynamic structures in a two-dimensional inhomogeneous plasma. *Physics of Plasmas*, 15(6):062308, 2008.
- [16] Sharad K. Yadav. Electron Magnetohydrodynamic (Emhd) Studies on Electron Transport in an Inhomogeneous Plasma Medium. *Thesis*.
- [17] Sharad Kumar Yadav, Amita Das, Predhiman Kaw, and Sudip Sengupta. Anomalous energy dissipation of electron current pulses propagating through an inhomogeneous collisionless plasma medium. *Physics of Plasmas*, 16(4):040701, 2009.
- [18] R. G. Hemker. Particle-In-Cell Modeling of Plasma-Based Accelerators in Two and Three Dimensions. *Thesis, University of California, Los Angeles*, 2000.
- [19] R. A. Fonseca, L. O. Silva, F. S. Tsung, V. K. Decyk, W. Lu, C. Ren, W. B. Mori, S. Deng, S. Lee, T. Katsouleas, and J. C. Adam. *OSIRIS: A Three-Dimensional, Fully Relativistic Particle in Cell Code for Modeling Plasma Based Accelerators*, pages 342–351. Springer Berlin Heidelberg, Berlin, Heidelberg, 2002.
- [20] R A Fonseca, S F Martins, L O Silva, J W Tonge, F S Tsung, and W B Mori. One-to-one direct modeling of experiments and astrophysical scenarios: pushing the envelope on kinetic plasma simulations. *Plasma Physics and Controlled Fusion*, 50(12):124034, 2008.
- [21] Tatsufumi Nakamura, Sergei V Bulanov, Timur Zh Esirkepov, and Masaki Kando. High-energy ions from near-critical density plasmas via magnetic vortex acceleration. *Physical review letters*, 105(13):135002, 2010.
- [22] Qing Jia, Kunioki Mima, Hong-bo Cai, Toshihiro Taguchi, Hideo Nagatomo, and X. T. He. Self-generated magnetic dipoles in weakly magnetized beam-plasma system. *Phys. Rev. E*, 91:023107, Feb 2015.
- [23] Tatsufumi Nakamura and Kunioki Mima. Magnetic-dipole vortex generation by propagation of ultraintense and ultrashort laser pulses in moderate-density plasmas. *Phys. Rev. Lett.*, 100:205006, May 2008.
- [24] Predhiman Kaw and John Dawson. Relativistic nonlinear propagation of laser beams in cold overdense plasmas. *The Physics of Fluids*, 13(2):472–481, 1970.
- [25] P.K. Kaw. Nonlinear laserplasma interaction. *Rev. Mod. Plasma Phys.*, 1, 2017.
- [26] J R Davies. Laser absorption by overdense plasmas in the relativistic regime. *Plasma Physics and Controlled Fusion*, 51(1):014006, dec 2008.
- [27] Y. Sentoku, K. Mima, P. Kaw, and K. Nishikawa. Anomalous resistivity resulting from mev-electron transport in overdense plasma. *Phys. Rev. Lett.*, 90:155001, Apr 2003.

Simulation Domain

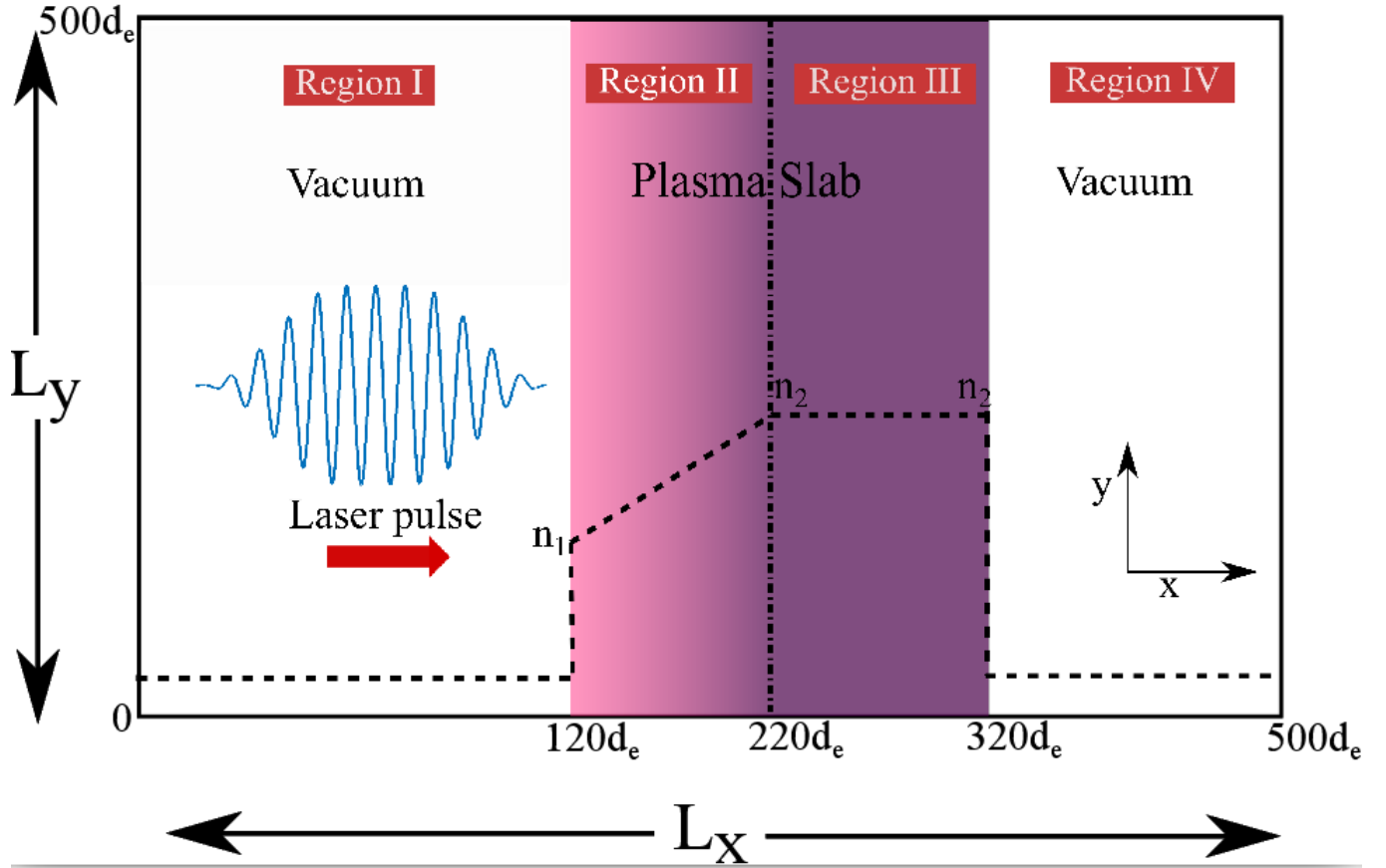


FIG. 1: Schematic of simulation setup(not to scale)used for this study. Simulation plane has been divided into four regions where Region I and IV are vacuum and region II and III contains plasma. A finite longitudinal and transverse extent intense pulse is incident on this plasma slab.

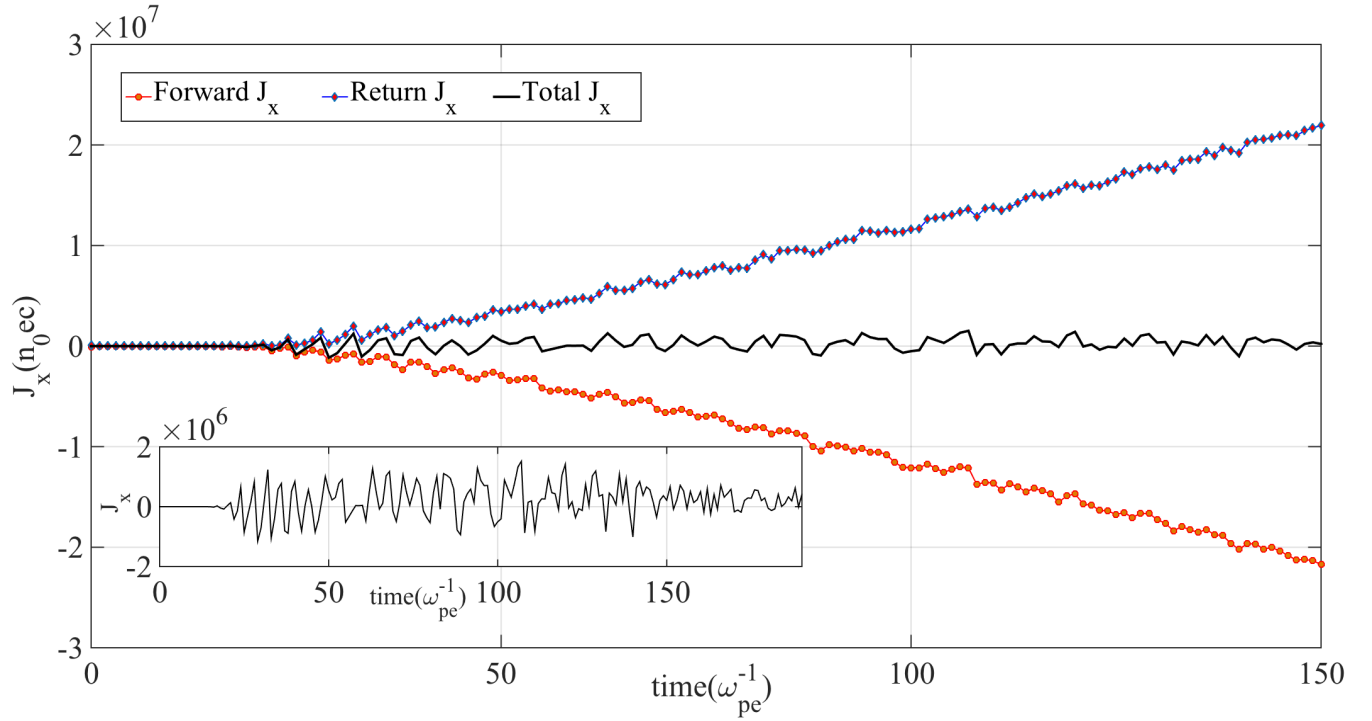


FIG. 2: Longitudinal current density evolution which is integrated over all the bulk plasma which interacts with focal spot of laser. Inset plot has only total electron J_x which is only one order less than forward and reverse current and mismatch remains persistent over 200 plasma periods.

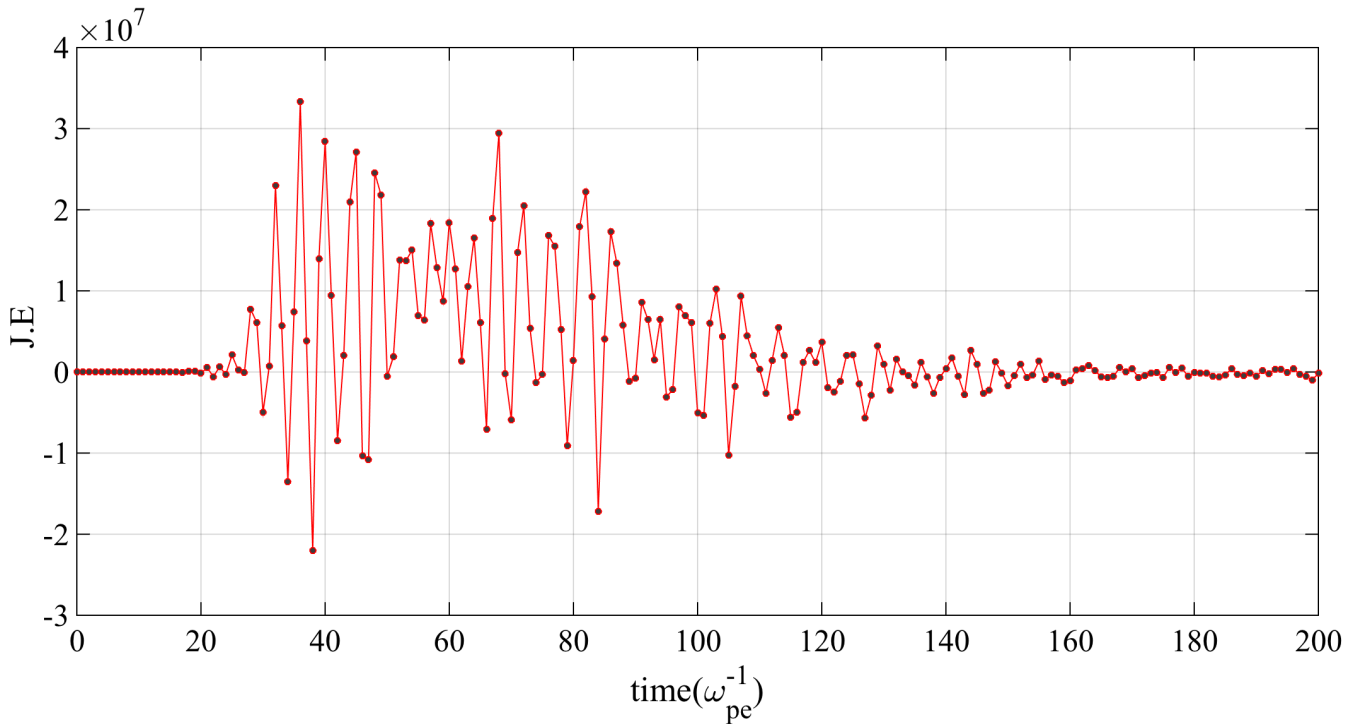


FIG. 3: Evolution of Integrated quantity $\vec{J} \cdot \vec{E}$ at every grid point of bulk plasma. Fluctuations in this plot establishes the uncompensation of current between the forward and return current.

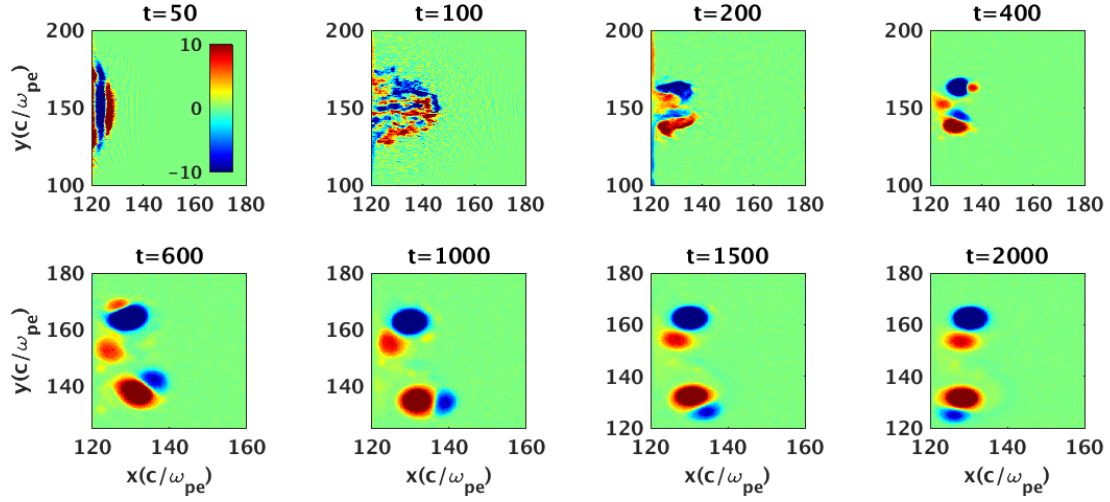


FIG. 4: Evolution of B_z where plasma slab has homogenous density profile i.e. $n = 10n_c$ from $x = 120$ to $x = 320$.

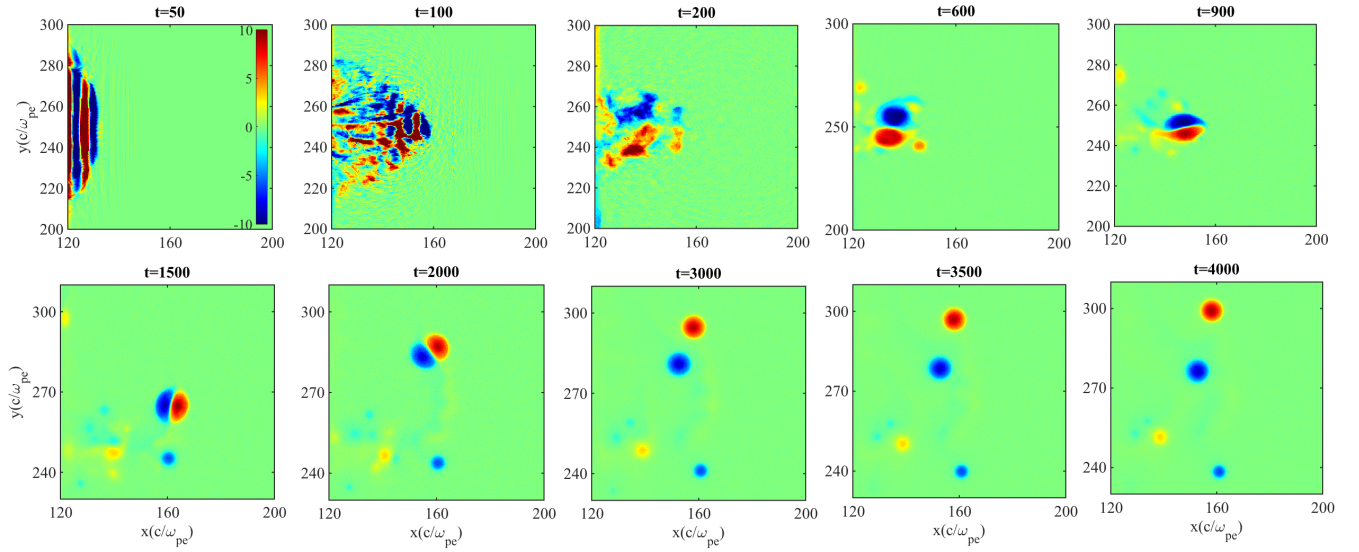


FIG. 5: Evolution of B_z where plasma slab has inhomogenous density profile i.e. $\delta n/\delta x = 0.05$ in region II along \hat{x} .

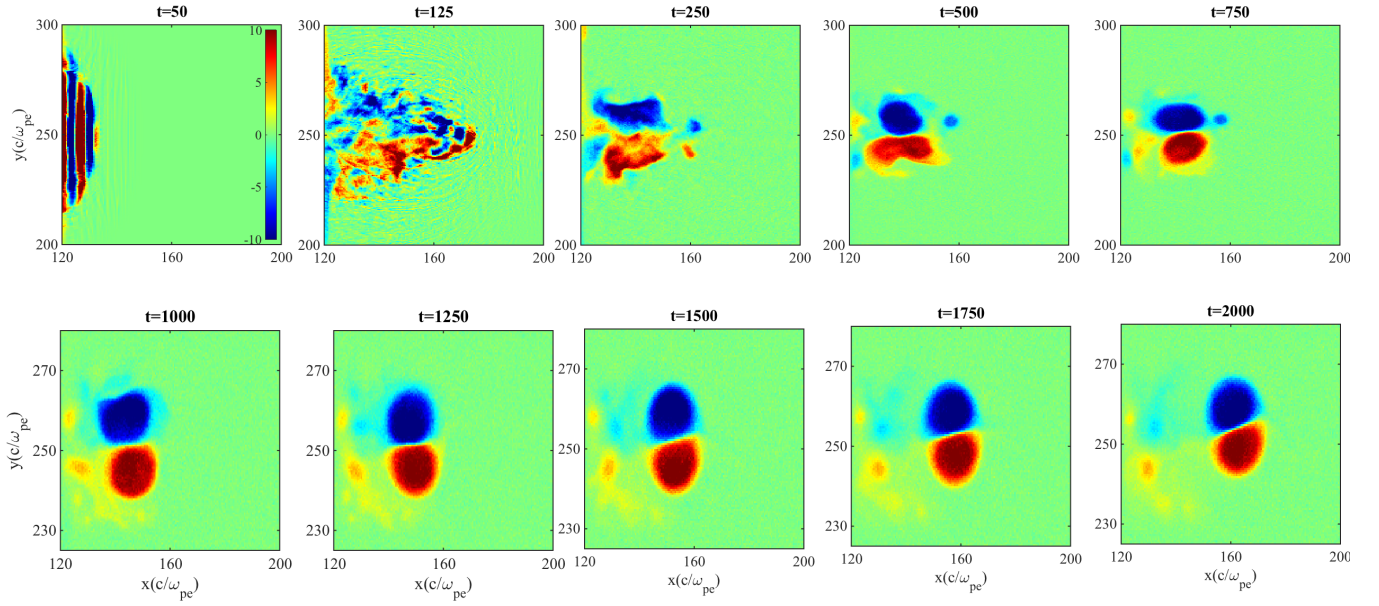


FIG. 6: Evolution of B_z where plasma slab has inhomogeneous density profile i.e. $\delta n/\delta x = 0.005$ in region II along \hat{x} .

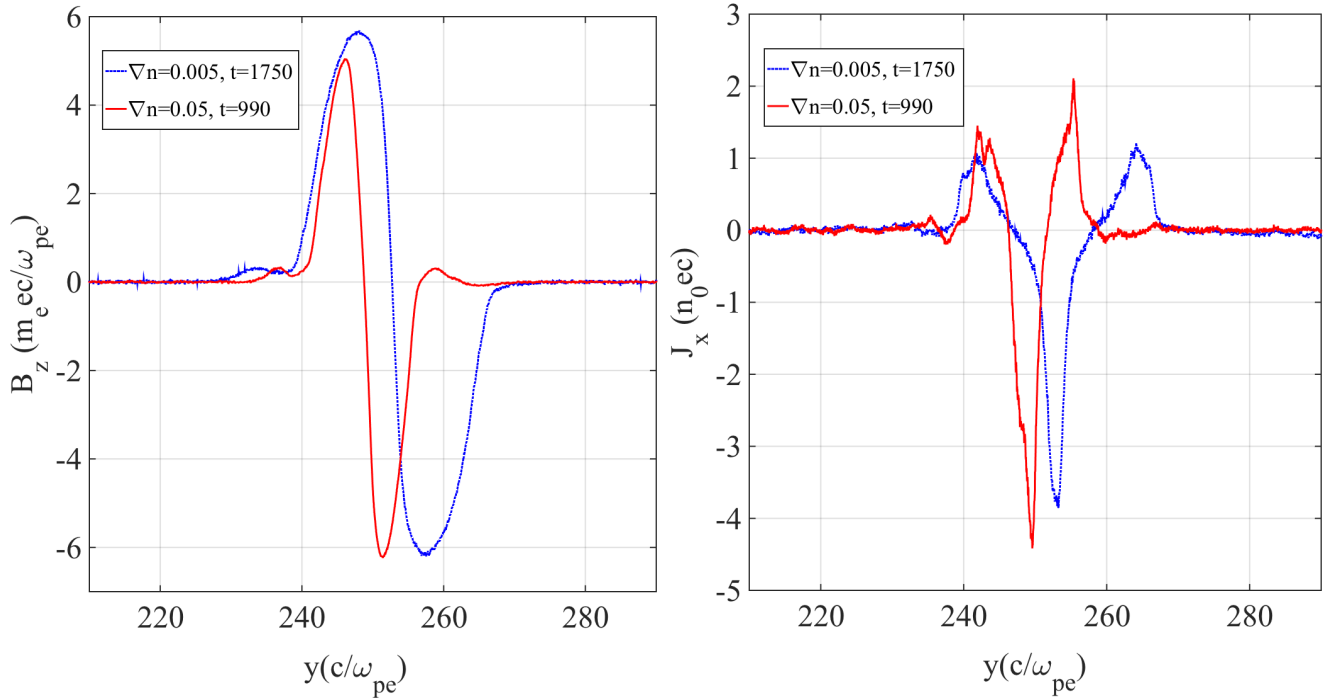


FIG. 7: Spatial variation of B_z and J_x for case(A) where $\delta n/\delta x = 0.05$ similarly for case(B) where $\delta n/\delta x = 0.005$ in region II. Time has been chosen when dipole has been formed and it has travelled in longitudinal direction but it is yet to turn in their trajectory. B_z and J_x for both cases has been plotted as function y .

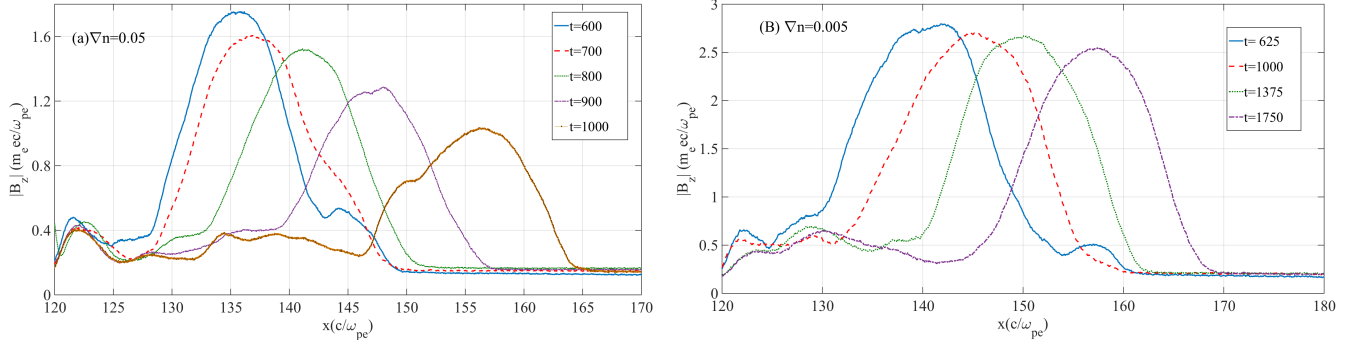


FIG. 8: Spatial variation of $\langle |B_z| \rangle$ for case(A) and case(B). Strength and translation of dipole is evident from these subplots, in case(A) dipole are not robust like in case(B). Average translation velocity is also higher in case(A).

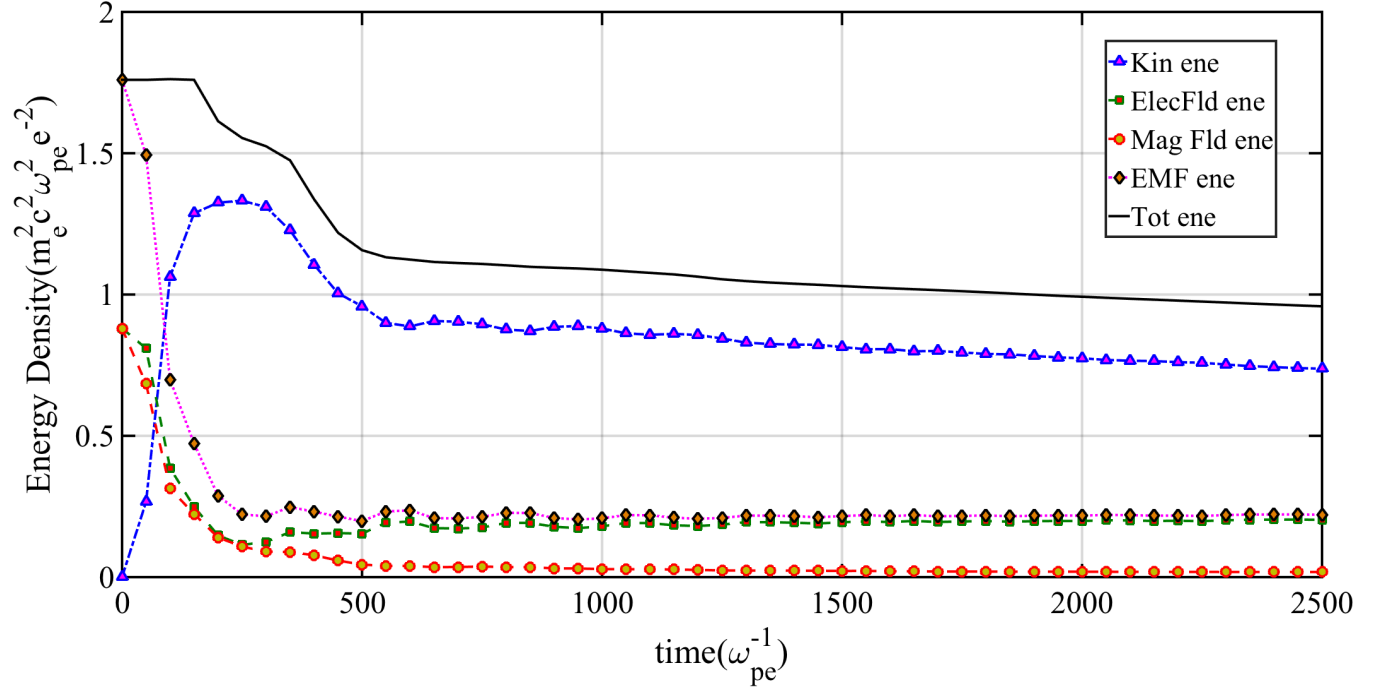


FIG. 9: Energy evolution where plasma density varies $\delta n / \delta x = 0.05$ in \hat{x} direction. The fall of EMF energy happens when laser pulse has completely left the simulation box and after $t \approx 500$ system establishes equilibrium.

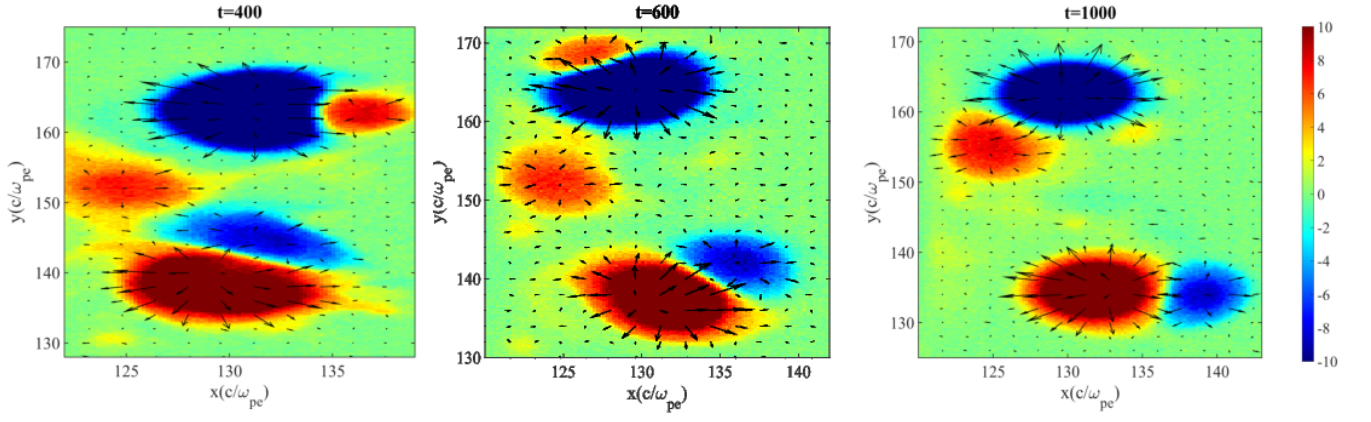


FIG. 10: Quiver plot of \vec{E} is being plotted over colorplot of B_z to show the effect of $\vec{E} \times \vec{B}$ in the homogenous case where $n = 10n_c$.

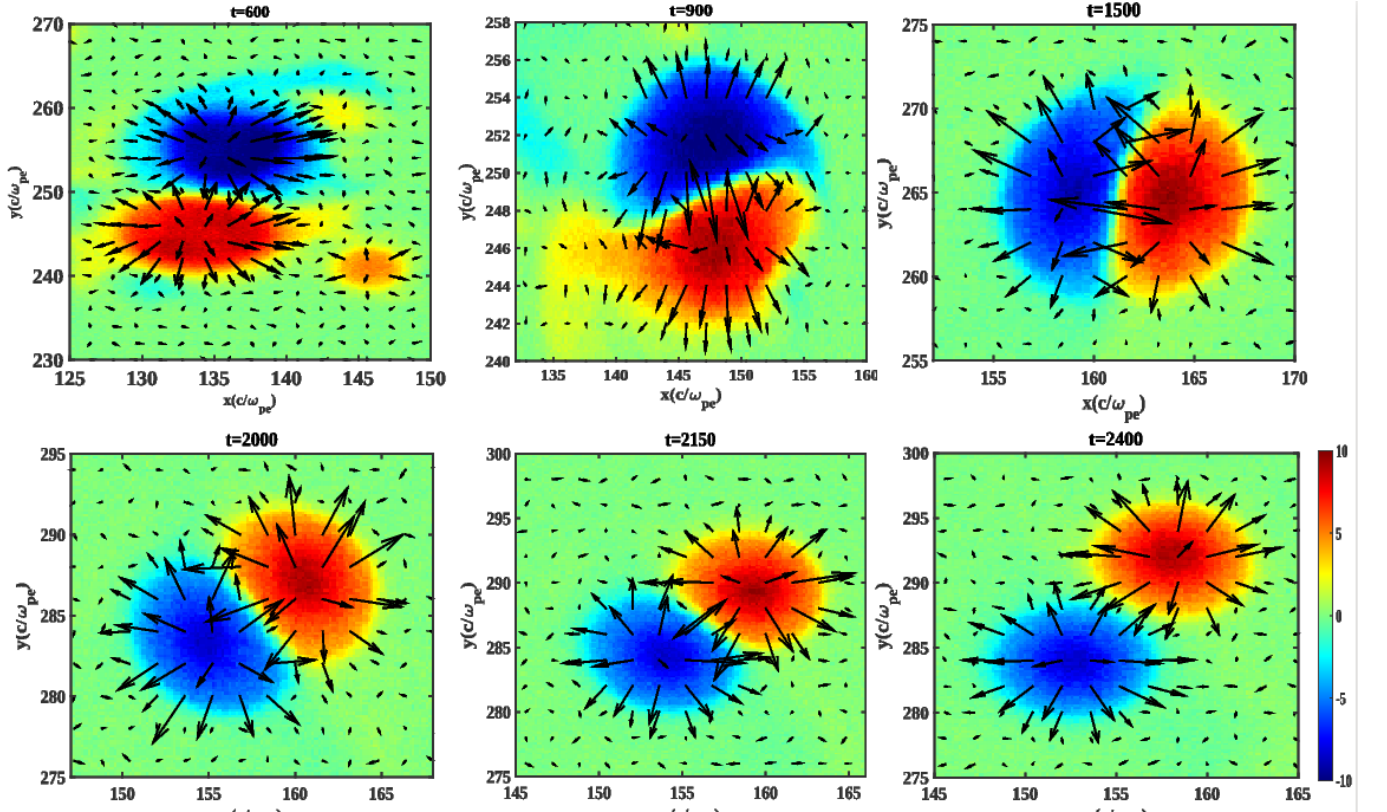


FIG. 11: Quiver plot of \vec{E} is being plotted over colorplot of B_z to show the effect of $\vec{E} \times \vec{B}$ in the inhomogenous case where $\delta n/\delta x = 0.05$.

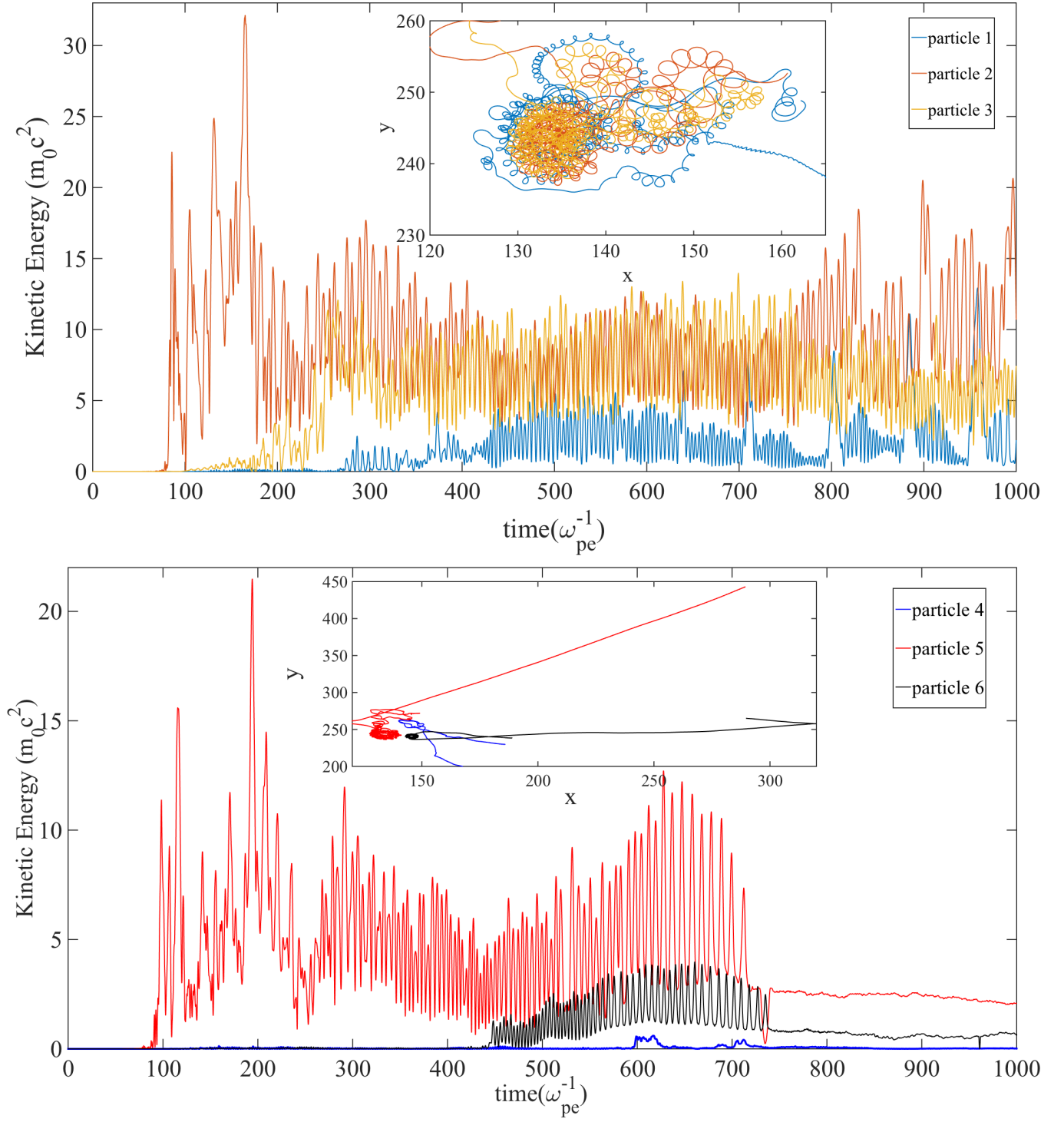


FIG. 12: Particle trajectories are plotted in inset of two subplots and each color represents a particular particle and its energy evolution with time has also been plotted.